

# On-surface stereoconvergent synthesis, dimerization and hybridization of organocopper complexes

Chi Zhang, Qiang Sun, Huihui Kong, Chunxue Yuan\* &amp; Wei Xu\*

*Interdisciplinary Materials Research Center, College of Materials Science and Engineering, Tongji University, Shanghai 201804, China*

Received June 12, 2018; accepted August 31, 2018; published online December 21, 2018

Despite the vital role of stereoconvergent synthesis in modern chemistry, the on-surface stereoconvergent synthesis of organometallic complexes involving transformation among several stereoisomers to one specific form has been few reported. By combination of high-resolution scanning tunneling microscopy (STM) imaging/manipulation and density functional theory (DFT) calculations, we have displayed the stereoconvergent synthesis of organocopper complexes via the Cu-alkene interaction and further dimerization into H-shaped motifs, in which two *cis*-forms and one *trans*-form are involved, and the specific adsorption configuration of one *cis*-form is revealed to be the key for such a synthesis. Furthermore, the generality of the dimerization of organocopper complexes has also been verified by codeposition of two similar molecular precursors, and the hybridized K-shaped motifs (made up of two kinds of organocopper complexes) have been successfully achieved. These findings may provide atomic-scale insights into the synthesis of specific stereoisomers in the fields of pharmaceuticals, biochemistry and organometallic chemistry.

**scanning tunneling microscopy, density functional theory, surface chemistry, organometallic complex, stereoconvergent synthesis**

**Citation:** Zhang C, Sun Q, Kong H, Yuan C, Xu W. On-surface stereoconvergent synthesis, dimerization and hybridization of organocopper complexes. *Sci China Chem*, 2019, 62: 126–132, <https://doi.org/10.1007/s11426-018-9355-8>

## 1 Introduction

Stereoconvergent synthesis, as one of the subordinate branches of asymmetric synthesis, has been aiming at full conversion of the stereoisomer mixture to one specific favored isomer [1–3]. Due to the dramatically different chemical or biological activities and applications among the corresponding stereoisomers, stereoconvergent synthesis is particularly vital and valuable in modern chemistry and has also been an urgent demand in selective synthesis [1,2]. Large numbers of studies [1,3–7] concerning such stereoconvergent reactions have been performed in traditional chemical syntheses, with high yields, selectivity and also enantiomeric excess. Nowadays, the increasingly developing

surface science methods make it possible to realize such reactions in a two-dimensional regime. Enormous efforts have been devoted to the controllable transformation between *cis* and *trans* isomers of azobenzene molecules (with N=N bonds) [8–13], alkene molecules (with C=C bonds) [14–16] by various means. More recently, the stereoselective synthesis of a specific *cis*-diene moiety on Cu(110) through a dehalogenative homocoupling strategy [17] was reported, while the corresponding *trans*-diene moiety was successfully synthesized via dehydrogenative homocoupling reaction on the same substrate [18]. In these on-surface reactions, the reaction products have been achieved with high stereoselectivity, yet, the stereoconvergent synthesis involving transformations among several stereoisomers to the specific one, to the best of our knowledge, has been few reported. Thus, it is particularly fascinating and also challenging to

\*Corresponding authors (email: [cyxuan@tongji.edu.cn](mailto:cyxuan@tongji.edu.cn); [xuwei@tongji.edu.cn](mailto:xuwei@tongji.edu.cn))

explore a system involving such kinds of stereoconvergent processes and gain reaction products with high stereo-purity, which may open up bright prospects towards on-surface formation of specific stereoisomers in a highly selective manner.

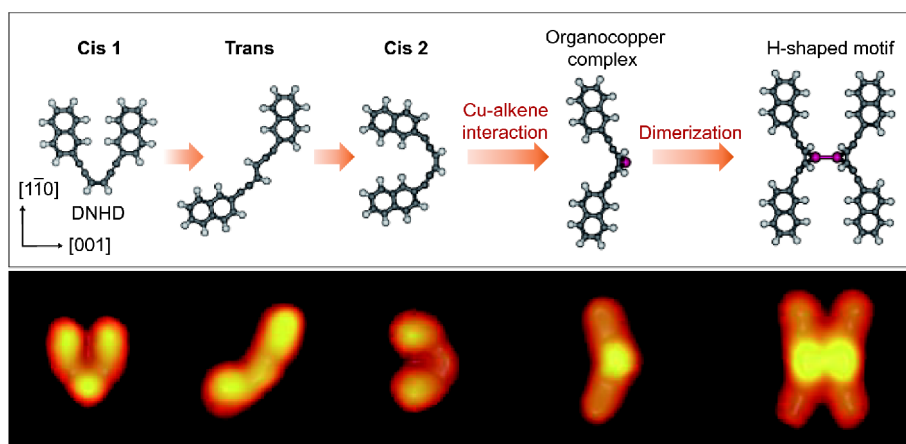
In this study, we design a system involving both organic molecules and metal atoms to explore the stereoconvergent synthesis of organometallic complexes. We choose a molecular precursor with an enediyne moiety (i.e., (*Z*)-1,6-di(naphthalen-2-yl)hexa-3-en-1,5-diyne, shortened as DNHD, as shown in Scheme 1) to enable the stereo-flexibility of carbon-carbon double bond (*cis-trans* isomerization) [14–16] and the potential metal-alkene interaction [19]. The Cu(110) surface is employed to provide a platform which enables a special adsorption configuration of the enediyne moiety compared to other surfaces, e.g., Ag(110) and Au(111), as we proposed before [19]. Besides, the availability of Cu adatoms is another consideration for the synthesis of organocopper complexes. From the interplay of high-resolution scanning tunneling microscopy (STM) imaging/manipulation and density functional theory (DFT) calculations, we have explored a sequential process involving the isomerization from **cis 1** through **trans** to **cis 2** followed by the formation of the organocopper complex and the final H-shaped motif, which thus shows the stereoconvergent synthesis of the specific H-shaped motif on the Cu(110) surface (cf. Scheme 1). The DFT calculations and STM simulations further allow us to confirm that such an H-shaped motif results from the dimerization of two identical organocopper complexes. Besides, the special adsorption configuration of the intermediate **cis 2** is revealed to be the key to facilitating the formation of the organocopper complex via Cu-alkene interaction. In such a process, high-yield conversion of the stereoisomers (**cis 1** and **trans**) to one specific favored **cis 2** isomer and then the H-shaped motif can be successfully achieved on the surface. To demonstrate the

generality on the formation and dimerization of organocopper complexes, we introduce another molecule (i.e., (*Z*)-1,6-bis(4-(*tert*-butyl)phenyl)hexa-3-en-1,5-diyne, shortened as BtPHD) together with DNHD molecule on the Cu(110) surface. More interestingly, we have also synthesized the “hybridized” K-shaped motif (which is made up of two kinds of organocopper complexes) together with the H-shaped (by the DNHD molecule) and X-shaped (by the BtPHD molecule) ones, respectively.

## 2 Experimental

All STM experiments were performed in a UHV chamber (base pressure  $1 \times 10^{-10}$  mbar) equipped with a variable-temperature, fast-scanning “Aarhus-type” STM using electrochemically etched W tips purchased from SPECS [20,21], a molecular evaporator and an e-beam evaporator, and other standard instrumentation for sample preparation. After the system was thoroughly degassed, the molecules were deposited by thermal sublimation onto a Cu(110) substrate. The sample was thereafter transferred within the UHV chamber to the STM, where measurements were usually carried out at  $\sim 150$  K. Only in the case of Figure 1(a, b), the STM images were obtained at room temperature (RT). All the STM images were further smoothed to eliminate noises. The lateral manipulations were carried out in a controllable line-scan mode under specific scanning conditions (by increasing the tunnel current up to approximately 2.0 nA while reducing the tunnel voltage down to approximately 20 mV) [22,23].

The calculations were performed in the framework of DFT by using the Vienna ab initio simulation package (VASP) [24,25]. The projector-augmented wave method was used to describe the interaction between ions and electrons [26,27]; the Perdew-Burke-Ernzerh of generalized gradient approximation exchange-correlation functional was employed [28],



**Scheme 1** Schematic illustration and the corresponding STM images showing the stereoconvergent synthesis of the specific H-shaped organocopper complex. Grey: C; white: H; wine: Cu. The substrate lattice direction is also shown (color online).

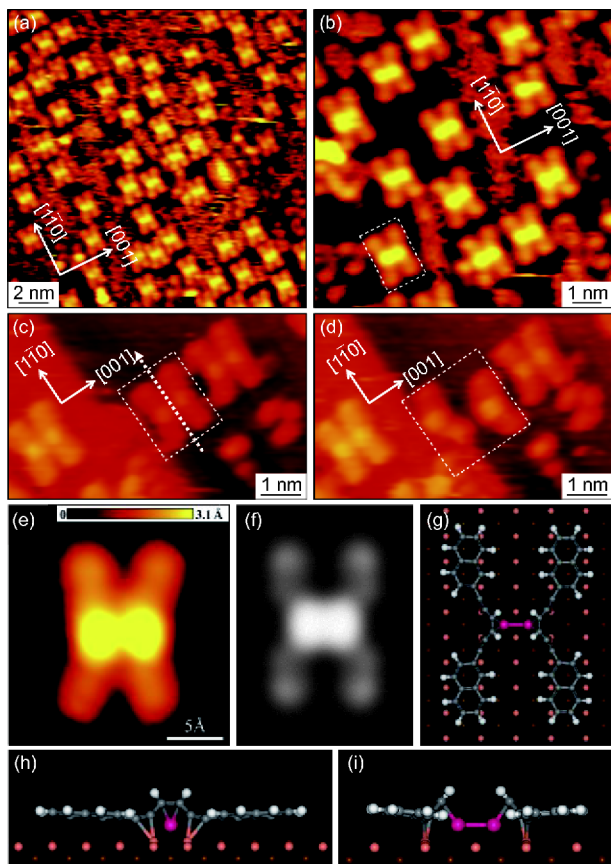


**Figure 1** Synthesis and dimerization of organocopper complexes on Cu(110) from DNHD molecules. (a) Large-scale and (b) close-up STM images showing the predominant formation of H-shaped motifs (as marked by the white rectangle) after deposition of DNHD molecules on a Cu(110) substrate held at RT (also scanned at RT). (c, d) Sequential STM images show the split of the H-shaped motif after lateral STM manipulations. The white arrow in (c) indicates the location and direction of the manipulation applied, and the white square in (d) highlights the two separated parts after manipulation. (e) High-resolution STM image and (f) simulated STM image of the H-shaped motif. (g–i) The top and side views of the corresponding DFT-optimized structural models of the H-shaped motif on Cu(110), respectively. Scanning condition: tunneling current  $I_t=0.60$  nA, bias voltage  $V_t=-2500$  mV (color online).

and van der Waals interactions were included using the dispersion-corrected DFT-D3 method of Grimme [29]. The atomic structures were relaxed using the conjugate gradient algorithm scheme as implemented in the VASP code until the forces on all unconstrained atoms were  $\leq 0.03$  eV/Å. Plane waves were used as a basis set with an energy cutoff of 400 eV for the models, and calculations were performed on a  $2 \times 2 \times 1$  k-point grid. Cu(110) surface was modeled by three-layered slabs for structural models of **cis 2** and three possible organocopper complexes, while two-layered slabs for structural models of H-shaped and K-shaped motifs (shown in the following figures). The simulated STM images were obtained by the Hive program based on the Tersoff-Hamann method [30,31].

### 3 Results and discussion

After deposition of the DNHD molecules on the Cu(110) substrate held at RT, we find the dominant formation of H-shaped motifs with a quite high yield (Figure 1(a)), and a typical one is marked by the rectangle shown in Figure 1(b). Such H-shaped motifs grow along the  $[1\bar{1}0]$  direction of the substrate. Moreover, each motif can diffuse as a whole on the surface (Figure S1, Supporting Information online), which implies the relatively strong bonding within one motif. To further investigate the constitution of the H-shaped motif, lateral STM manipulation has been performed on it (Figure 1(c)), which can be split along the  $[001]$  direction of the substrate into two identical bow-shaped parts (Figure 1(d)). The submolecularly resolved STM image of the H-shaped motif (Figure 1(e)) shows that it is made up of two bow shapes with two distinguishable bright protrusions at the center. Such phenomenon is similar to that of the X-shaped motif (synthesized from another molecule BtPHD) [19] as reported previously, where each enediyne moiety can interact with one Cu atom via Cu-alkene interaction forming the organocopper complex and then dimerization into the X-shaped motif via Cu-Cu interaction. It is also known that Cu adatoms are available on Cu(110) at RT [19,32].

Inspired from that and on the basis of the STM topography and dimension, we propose that the H-shaped motif should be made up of two DNHD molecules and two Cu adatoms. We have optimized several structural models by DFT calculations and obtained the most favorable structural model as shown in Figure 1(g–i) (detailed in Figure S2). From the models, it is confirmed that the H-shaped motif is formed by dimerization of two organocopper complexes via Cu-Cu interaction. Each organocopper complex is synthesized by one *cis*-form DNHD molecule interacting with one Cu adatom (positioned under the alkene group) via Cu-alkene bonding, resulting in the nearly tetrahedral bonding configuration of the alkene moiety and thus from  $sp^2$  to  $sp^3$  rehybridization characteristics. Then, the strongly tilted enediyne part appears as the characteristic bright protrusion in the STM image, which is in good accordance with the corresponding simulated STM image (Figure 1(f)). What's more, the existence of distorted H-shaped motif owing to the mismatch in the two neighboring organocopper complexes (Figure S3) also rationalizes the dimerization of two organocopper complexes.

From the model shown in Figure 1(g), we can clearly observe that the configuration of DNHD molecules in the H-shaped motif is dramatically different from the low-temperature adsorption configuration of the DNHD molecule on the Cu(110) surface, which is, for example, shown in Figure 2(a). In order to experimentally identify the possible intermediates, we have systematically studied the evolution process of the DNHD molecules on Cu(110) by stepwise

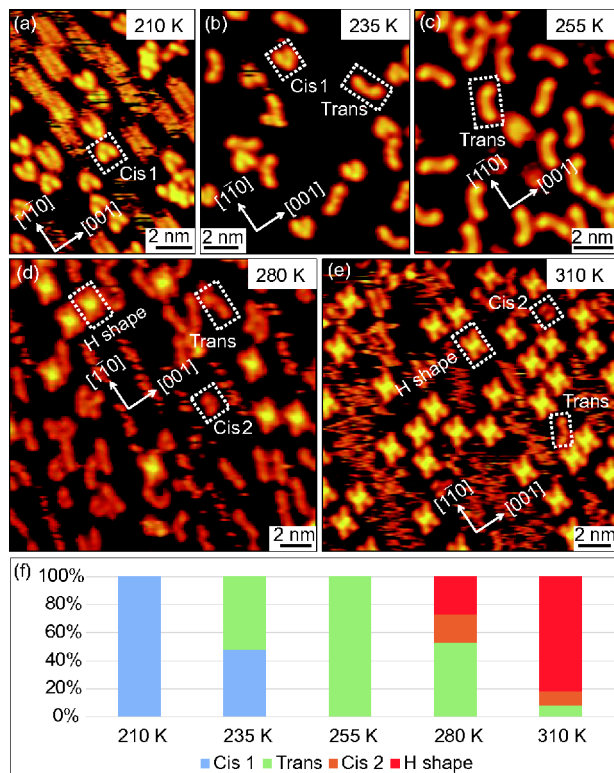


**Figure 2** Identification of the evolution process of DNHD molecules on Cu(110) in response to the different annealing temperatures. (a–e) STM images obtained after (a) deposition of DNHD molecules on the Cu(110) substrate held at  $\sim 210$  K; (b) annealing at  $\sim 235$  K for 10 min; (c) annealing at  $\sim 255$  K for 10 min; (d) annealing at  $\sim 280$  K for 10 min; (e) annealing at  $\sim 310$  K for 10 min. Scanning condition:  $I_t=0.50$  nA,  $V_f=-2500$  mV. (f) Statistical diagram displaying the evolution process and the corresponding percentages of constituents in the annealing temperature range from 210 to 310 K (color online).

regulation of the annealing temperatures. As we have shown before [14,33,34], deposition of the DNHD molecules on Cu(110) held at  $\sim 210$  K or below (Figure 2(a)) results in the *cis*-form adsorption configuration, which is assigned to **cis 1** here (cf. Scheme 1). Thermal treatment in the range of  $\sim 210$ – $255$  K leads to the gradual **cis 1**-**trans** isomerization (Figure 2(b, c)). At this state, there is still no indication of the H-shaped motif.

After further annealing to  $\sim 280$  K, the H-shaped motifs start to appear as shown in Figure 2(d), and meanwhile, unexpectedly, we find another *cis*-form (assigned to **cis 2**, also refer to Scheme 1) with the symmetric axis along the [001] direction of the substrate, i.e.,  $90^\circ$  rotation from the **cis 1**. Such samples have been achieved at different molecular coverages (Figure S4). When annealing to  $\sim 310$  K, the H-shaped motifs become dominant with a relatively high yield (Figure 2(e)), and both **trans** and **cis 2** drastically decrease. From the detailed statistics (Figure 2(f)), we can observe the tendency in the evolution process where the decrease of **trans** promotes the formation of both **cis 2** and H-shaped motifs at first, and then H-shaped motifs are further con-

structed at the cost of both **trans** and **cis 2**.

Now, the first attractive question arises: how is the H-shaped motif constructed? As shown in Figure 1(a, b), such H-shaped motifs specifically grow along the [1 $\bar{1}$ 0] direction of the substrate; moreover, the motif can only be split along the [001] direction (Figure 1(d)), which indicates that the H-shaped motif is most probably constructed by the **cis 2** rather than the **trans**. This is because: (1) the **trans** has no specific adsorption direction (Figure 2(c)), and such kind of metal-alkene interaction should normally occur between metals and **cis**-forms as extensively reported in the field of organometallic chemistry [35,36]; (2) **cis 2** just has the coincident adsorption direction with the symmetric axis along the [001] direction. Then, the next question is what the relation is among **cis 1**, **trans**, and **cis 2**? To *in-situ* figure out this question, we have again performed lateral STM manipulations on **cis 2**. As shown in Figure 3(a, b), interestingly, **cis 2** can be manipulated to **cis 1** by doing a line-scan along the [1 $\bar{1}$ 0] direction. Besides, **cis 2** can also be manipulated to **trans** by doing a line-scan along the [001] direction (cf. Figure S5(a, b)). Since **cis 1** and **cis 2** are intrinsically the same *cis* structure of DNHD molecule just with different adsorption directions with respect to the substrate lattice, the third question then arises: why all of the H-shaped motifs are along the [1 $\bar{1}$ 0] direction? In other words, the H-shaped motif

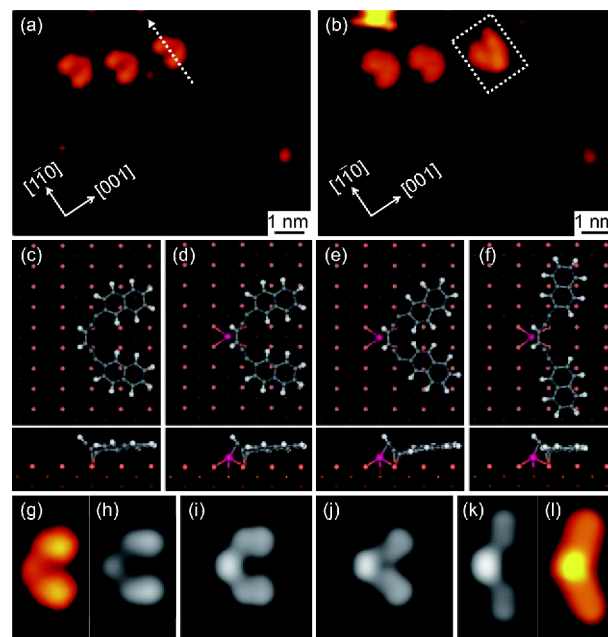


**Figure 3** (a, b) Lateral STM manipulation on one **cis 2** structure showing the transformation from **cis 2** to **cis 1**. The arrow in (a) indicates the location and direction of the manipulation applied, and the rectangle in (b) highlights the evolution of the target structure. (c–f) Top and side views of the DFT-calculated structural models of (c) **cis 2** and (d–f) three possible organocopper complexes on Cu(110). (g, h) High-resolution STM image and the simulated STM image of **cis 2**, respectively. (i–k) The simulated STM images corresponding to the structural models shown in (d–f), respectively. (l) The high-resolution STM image of the remaining half of the H-shaped motif obtained after STM manipulation (color online).

is only made up of **cis 2** rather than **cis 1**. Note that at the substrate temperatures above 200 K, Cu adatoms already prevail on the Cu(110) surface. So, the temperature is not an issue.

In order to unravel the underlying mechanism, we have performed DFT calculations on the structure search of **cis 2**. From the high-resolution STM image (Figure 3(g)), we can see that **cis 2** seems a little bit smaller than **cis 1**. On the basis of the STM topography and adsorption direction, we have obtained the on-surface structural model of **cis 2** (Figure 3(c)) and the corresponding simulated STM image (Figure 3(h)). From the structural model (Figure 3(c)), astonishingly, we distinguish that **cis 2** adopts a different adsorption geometry from **cis 1**, that is, the enediyne moiety is tilted due to the interactions with the substrate. In comparison with the flat-lying adsorption configuration of **cis 1** [34], only **cis 2** can adopt this special configuration which thus facilitates the Cu-alkene interaction, in accordance with what we have proposed for another molecular system [19].

Experimentally, we found **cis 2** and H-shaped motifs always coexist. **cis 2** is calculated to be energetically less favorable than **trans** by 0.75 eV. Besides, **trans** was calculated to be more stable than **cis 1** by 0.28 eV [14]. This means **cis 2** is just an intermediate state towards the formation of the organocopper complex. Accordingly, we perform further DFT calculations to figure out the structural model of the organocopper complex. As is known, the Cu adatom may go underneath the tilted enediyne moiety by forming the Cu-alkene interaction. Then three possible structural models for organocopper complex are built up and shown in Figure 3(d–f), and the corresponding simulated STM images are shown in Figure 3(i–k). After directly interacting with Cu adatom (Figure 3(d)), the structure becomes energetically more stable by 0.32 eV. It can be observed that the naphthalene rings can flip during the formation of *trans* (Figure S6), and two kinds of *trans*-forms (arc-shaped and S-shaped) with the naphthalene rings flipped have been found to coexist. Also, from the sequential STM images scanned at the same region (Figure S5(b, c)), we can observe the spontaneous conformational changes between these two *trans*-forms. Similar conformational changes with the functional groups flipped [37–39] have also been reported previously. Then, we have also optimized one structural model with the naphthalene rings flipped (cf. Figure 3(e)), and it is calculated to be more stable than that shown in Figure 3(d) by 0.23 eV. However, the corresponding simulated STM image (Figure 3(j)) does not agree with the experimental STM topography (i.e., half of the H-shaped motif gained via STM manipulation) (Figure 3(l)), which may be due to the steric hindrance between two neighboring naphthalene rings. Then, according to the STM topography, we have relaxed another structure by further expanding two naphthalene rings (Figure 3(f)), and the corresponding STM simulation (Figure 3(k)) resembles the

experimental one (Figure 3(l)) very well. This structure is energetically more stable than that shown in Figure 3(e) by 0.17 eV. The detailed energy diagram of this process is shown in Figure S7. On the basis of these DFT calculations together with the relevant literatures [19,40], the formation of the organocopper complex is rationalized.

It is noteworthy that the reason we propose such a process as stereoconvergent synthesis is that the starting state can be the **cis 1** form ( $T \leq 210$  K, Figure 2(a)) or the **trans** form ( $T \sim 255$  K, Figure 2(c)), or even the mixture of both **cis 1** and **trans** forms ( $210 \text{ K} < T < 255 \text{ K}$ , Figure 2(b)). Based on any of these stereodivergent starting isomers, they can be transformed to the specific **cis 2** form and then form the H-shaped organocopper complexes by combining with Cu adatoms and further dimerization. In this way, full conversion of the stereoisomer mixture to one specific favored isomer [1–3] can be successfully achieved on the surface.

As a step further, to demonstrate the generality of the synthesis and dimerization of organocopper complexes, we have codeposited two similar molecular precursors (i.e., DNHD and BtPHD molecules) on the Cu(110) surface. As shown in Figure 4(a), both molecules have the enediyne moieties that enable them to interact with the Cu adatoms by forming different organocopper complexes. After codeposition of DNHD and BtPHD molecules on a Cu(110) substrate held at RT, as expected, we observe a few K-shaped motifs (by hybridization of DNHD and BtPHD molecules) coexisting with H-shaped (by DNHD molecules) and X-shaped [19] (by BtPHD molecules) ones as shown in Figure 4(b, c), which presents the possibility of “hybridized” dimerization from similar organocopper complexes. High-resolution STM image (Figure 4(d)) shows that the K-shaped motif has the characteristics of both H-shaped and X-shaped ones with two bright protrusions at the center. The adsorption geometry on Cu(110) (Figure 4(f–h)) shows that the tilted enediyne moieties with Cu atoms underneath are attributed to the bright protrusions (similar to the situations in both H-shaped and X-shaped ones). The corresponding STM simulation (Figure 4(e)) further exhibits a similar profile to the experimental data. Furthermore, STM manipulations on K-shaped motifs also show that they can be split along the [001] direction of the substrate (Figure S8).

Thus, it is reasonable to reach the conclusion about the structure and construction of the H-shaped motif based on the following clues: (1) the formation of hybridized K-shaped motif; (2) STM manipulations on the H-shaped motif (Figure 1(c, d)) and the **cis 2** (Figures 3(a, b) and S4); (3) DFT calculations and related STM simulations; (4) control experiments of BtPHD on Ag(110) and Au(111), and STM manipulations on half of the X-shaped motif in our previous study [19]; (5) some literature supports involving both on-surface research [40] and studies in the field of organometallic chemistry [35,36].

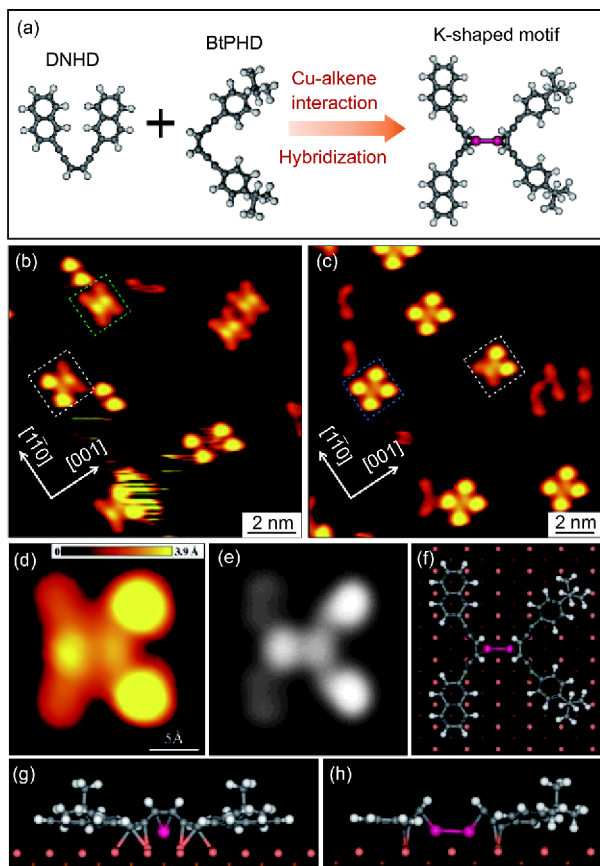


**Figure 4** Synthesis and dimerization of organocopper complexes on Cu(110) from both DNHD and BtPHD molecules. (a) Schematic illustration showing the hybridization of two organocopper complexes forming the K-shaped motif. (b, c) STM images showing the formation of hybridized K-shaped motifs (marked by white squares) together with H-shaped and X-shaped ones (marked by green and blue squares, respectively) after codeposition of DNHD and BtPHD molecules on a Cu(110) substrate held at RT. (d) High-resolution STM image of the K-shaped motif. Scanning condition:  $I_s=0.50$  nA,  $V_s=-2500$  mV. (e) The simulated STM image of the K-shaped one. (f–h) The top and side views of the DFT-optimized structural models of the K-shaped motif on Cu(110) (color online).

## 4 Conclusions

In conclusion, by combination of high-resolution STM imaging/manipulation and DFT calculations, we have shown the stereoconvergent synthesis of organocopper complexes via Cu-alkene interaction and further dimerization with relatively high yields, in which the specific adsorption configuration of the enediyne moiety is revealed to be the key for such a process. Furthermore, the generality of dimerization between two similar organocopper complexes is presented. These findings demonstrate an example of the on-surface stereoconvergent synthesis of organocopper complexes, which may provide atomic-scale insights into the synthesis of specific stereoisomers with high selectivity in the relevant fields such as pharmaceuticals and biochemistry.

**Acknowledgements** This work was supported by the National Natural

Science Foundation of China (21473123, 21622307, 21790351), and the Fundamental Research Funds for the Central Universities. Prof. Aiguo Hu and Dr. Zhiwen Li are acknowledged for providing the molecules.

**Conflict of interest** The authors declare that they have no conflict of interest.

**Supporting information** The supporting information is available online at <http://chem.scichina.com> and <http://link.springer.com/journal/11426>. The supporting materials are published as submitted, without typesetting or editing. The responsibility for scientific accuracy and content remains entirely with the authors.

- Bhat V, Welin ER, Guo X, Stoltz BM. *Chem Rev*, 2017, 117: 4528–4561
- Park JK, Lackey HH, Ondrusek BA, McQuade DT. *J Am Chem Soc*, 2011, 133: 2410–2413
- Ito H, Kunii S, Sawamura M. *Nat Chem*, 2010, 2: 972–976
- Keylor MH, Matsuura BS, Griesser M, Chauvin JPR, Harding RA, Kirillova MS, Zhu X, Fischer OJ, Pratt DA, Stephenson CRJ. *Science*, 2016, 354: 1260–1265
- Lundin PM, Fu GC. *J Am Chem Soc*, 2010, 132: 11027–11029
- Guzman-Martinez A, Hoveyda AH. *J Am Chem Soc*, 2010, 132: 10634–10637
- Zhong C, Kunii S, Kosaka Y, Sawamura M, Ito H. *J Am Chem Soc*, 2010, 132: 11440–11442
- Aleman M, Peters MV, Hecht S, Rieder KH, Moresco F, Grill L. *J Am Chem Soc*, 2006, 128: 14446–14447
- Henzl J, Mehlhorn M, Gawronski H, Rieder KH, Morgenstern K. *Angew Chem Int Ed*, 2006, 45: 603–606
- Bazarnik M, Henzl J, Czajka R, Morgenstern K. *Chem Commun*, 2011, 47: 7764–7766
- Kazuma E, Han M, Jung J, Oh J, Seki T, Kim Y. *J Phys Chem Lett*, 2015, 6: 4239–4243
- Pechenezhskiy IV, Cho J, Nguyen GD, Berbil-Bautista L, Giles BL, Poulsen DA, Fréchet JMJ, Crommie MF. *J Phys Chem C*, 2012, 116: 1052–1055
- Xu LP, Wan LJ. *J Phys Chem B*, 2006, 110: 3185–3188
- Sun Q, Zhang C, Wang L, Li Z, Hu A, Tan Q, Xu W. *Chem Commun*, 2014, 50: 1728–1730
- Liao L, Li Y, Zhang X, Geng Y, Zhang J, Xie J, Zeng Q, Wang C. *J Phys Chem C*, 2014, 118: 15963–15969
- Tsai CS, Wang JK, Skodje RT, Lin JC. *J Am Chem Soc*, 2005, 127: 10788–10789
- Sun Q, Cai L, Ma H, Yuan C, Xu W. *Chem Commun*, 2016, 52: 6009–6012
- Sun Q, Cai L, Ding Y, Xie L, Zhang C, Tan Q, Xu W. *Angew Chem Int Ed*, 2015, 54: 4549–4552
- Zhang C, Sun Q, Kong H, Wang L, Tan Q, Xu W. *Chem Commun*, 2014, 50: 15924–15927
- Besenbacher F. *Rep Prog Phys*, 1996, 59: 1737–1802
- Laegsgaard E, Österlund L, Thosttrup P, Rasmussen PB, Stensgaard I, Besenbacher F. *Rev Sci Instrum*, 2001, 72: 3537–3542
- Xu W, Kong H, Zhang C, Sun Q, Gersen H, Dong L, Tan Q, Laegsgaard E, Besenbacher F. *Angew Chem Int Ed*, 2013, 52: 7442–7445
- Yu M, Xu W, Benjalal Y, Barattin R, Laegsgaard E, Stensgaard I, Hliwa M, Bouju X, Gourdon A, Joachim C, Linderoth TR, Besenbacher F. *Nano Res*, 2009, 2: 254–259
- Kresse G, Hafner J. *Phys Rev B*, 1993, 48: 13115–13118
- Kresse G, Furthmüller J. *Phys Rev B*, 1996, 54: 11169–11186
- Blöchl PE. *Phys Rev B*, 1994, 50: 17953–17979
- Kresse G, Joubert D. *Phys Rev B*, 1999, 59: 1758–1775
- Perdew JP, Burke K, Ernzerhof M. *Phys Rev Lett*, 1996, 77: 3865–3868
- Grimme S, Antony J, Ehrlich S, Krieg H. *J Chem Phys*, 2010, 132:

- 154104
- 30 Tersoff J, Hamann DR. *Phys Rev B*, 1985, 31: 805–813
- 31 Vanpoucke DEP, Brocks G. *Phys Rev B*, 2008, 77: 241308
- 32 Lee J, C.~Sorescu D, Lee JG, Dougherty D. *Surf Sci*, 2016, 652: 82–90
- 33 Sun Q, Zhang C, Li Z, Kong H, Tan Q, Hu A, Xu W. *J Am Chem Soc*, 2013, 135: 8448–8451
- 34 Sun Q, Zhang C, Li Z, Sheng K, Kong H, Wang L, Pan Y, Tan Q, Hu A, Xu W. *Appl Phys Lett*, 2013, 103: 013103
- 35 Crabtree RH. *The Organometallic Chemistry of the Transition Metals*. New Jersey: Wiley, 2005. 125–158
- 36 Love RA, Koetzle TF, Williams GJB, Andrews LC, Bau R. *Inorg Chem*, 1975, 14: 2653–2657
- 37 Weigelt S, Busse C, Petersen L, Rauls E, Hammer B, Gothelf KV, Besenbacher F, Linderoth TR. *Nat Mater*, 2006, 5: 112–117
- 38 Sánchez-Sánchez C, Nicolaï A, Rossel F, Cai J, Liu J, Feng X, Müllen K, Ruffieux P, Fasel R, Meunier V. *J Am Chem Soc*, 2017, 139: 17617–17623
- 39 Ammon M, Sander T, Maier S. *J Am Chem Soc*, 2017, 139: 12976–12984
- 40 Weber PB, Hellwig R, Paintner T, Lattelais M, Paszkiewicz M, Casado Aguilar P, Deimel PS, Guo Y, Zhang YQ, Allegretti F, Papa-georgiou AC, Reichert J, Klyatskaya S, Ruben M, Barth JV, Bocquet ML, Klappenberger F. *Angew Chem Int Ed*, 2016, 55: 5754–5759